

# Post-Synthetic Reversible Incorporation of Organic Linkers into Porous Metal–Organic Frameworks through Single-Crystal-to-Single-Crystal Transformations and Modification of Gas-Sorption Properties

Hye Jeong Park, Young Eun Cheon, and Myunghyun Paik Suh\*<sup>[a]</sup>

**Abstract:** The porous metal–organic framework (MOF)  $\{[\text{Zn}_2(\text{TCPBDA})(\text{H}_2\text{O})_2] \cdot 30\text{DMF} \cdot 6\text{H}_2\text{O}\}_n$  (**SNU-30**; DMF = *N,N*-dimethylformamide) has been prepared by the solvothermal reaction of *N,N,N',N'*-tetrakis(4-carboxyphenyl)biphenyl-4,4'-diamine ( $\text{H}_4\text{TCPBDA}$ ) and  $\text{Zn}(\text{NO}_3)_2 \cdot 6\text{H}_2\text{O}$  in DMF/*t*BuOH. The post-synthetic modification of **SNU-30** by the insertion of 3,6-di(4-pyridyl)-1,2,4,5-tetrazine (bpta) affords single-crystalline  $\{[\text{Zn}_2(\text{TCPBDA})(\text{bpta})] \cdot 23\text{DMF} \cdot 4\text{H}_2\text{O}\}_n$  (**SNU-31SC**), in which channels are divided by the bpta linkers. Interestingly,

unlike its pristine form, the bridging bpta ligand in the MOF is bent due to steric constraints. **SNU-31** can be also prepared through a one-pot solvothermal synthesis from  $\text{Zn}^{\text{II}}$ ,  $\text{TCPBDA}^{4-}$ , and bpta. The bpta linker can be liberated from this MOF by immersion in *N,N*-diethylformamide (DEF) to afford the single-crystalline **SNU-30SC**, which

is structurally similar to **SNU-30**. This phenomenon of reversible insertion and removal of the bridging ligand while preserving the single crystallinity is unprecedented in MOFs. Desolvated solid **SNU-30'** adsorbs  $\text{N}_2$ ,  $\text{O}_2$ ,  $\text{H}_2$ ,  $\text{CO}_2$ , and  $\text{CH}_4$  gases, whereas desolvated **SNU-31'** exhibits selective adsorption of  $\text{CO}_2$  over  $\text{N}_2$ ,  $\text{O}_2$ ,  $\text{H}_2$ , and  $\text{CH}_4$ , thus demonstrating that the gas adsorption properties of MOF can be modified by post-synthetic insertion/removal of a bridging ligand.

**Keywords:** bridging ligands • crystal engineering • gas sorption • metal–organic frameworks • synthetic methods

## Introduction

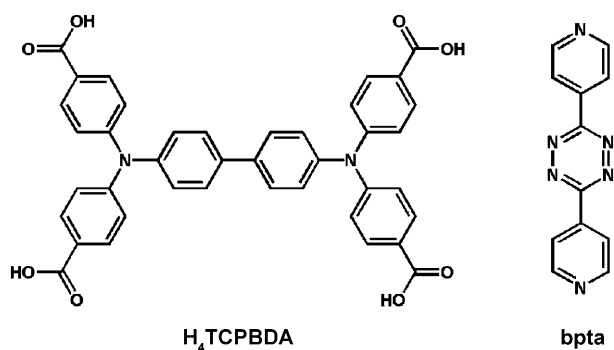
Porous metal–organic frameworks (MOFs) have attracted great attention because they can be applied in gas storage<sup>[1,2]</sup> and separation,<sup>[3]</sup> catalysis,<sup>[4]</sup> and fabrication of metal nanoparticles.<sup>[2a,5,6]</sup> The gas-sorption properties of a MOF, such as the type of adsorbed gases and the adsorption capacities, depend on the pore size and pore shape of the MOF, gas framework interactions, and gas–gas interactions. To change the pore size and pore shape, in general, new MOFs should be prepared by using a solvothermal reaction with different metal and/or organic building blocks. Recently, post-syntheses have been developed to functionalize MOFs.<sup>[7]</sup> If the

pore size and pore shape of a MOF can be controlled by post-synthetic methods, for example, by the insertion or removal of organic linkers, the selectivity of adsorbed gases and the gas uptake capacities could be easily modified. In addition, the MOFs that transform their structures in response to external stimuli by single-crystal-to-single-crystal (SCSC) transformations are important for the development of new and technologically useful devices and sensors. Even though a considerable number of studies have been reported on SCSC transformations of MOFs,<sup>[6,8–11]</sup> to the best of our knowledge, there has been no report of SCSC transformations on the insertion or removal of the organic framework component in a 3D MOF crystal, which alters the gas-sorption properties of the MOF.

Herein, we report the unprecedented post-synthetic reversible incorporation of bridging ligands in a MOF through SCSC transformations. Interestingly, the bridging ligand 3,6-di(4-pyridyl)-1,2,4,5-tetrazine (bpta), which is linear in the pristine form, is significantly bent in the present MOF due to steric constraints. The insertion of the organic linker alters the pore size and pore shape, thus significantly changing the gas-sorption properties of the MOF.

[a] H. J. Park, Y. E. Cheon, Prof. M. P. Suh  
Department of Chemistry  
Seoul National University  
Seoul 151-747 (Republic of Korea)  
Fax: (+82)28868516  
E-mail: mpsuh@snu.ac.kr

Supporting information for this article is available on the WWW under <http://dx.doi.org/10.1002/chem.201001549>.



## Results and Discussion

**Preparation and X-ray crystal structure studies of  $\{[\text{Zn}_2(\text{TCPBDA})(\text{H}_2\text{O})_2]\cdot 30\text{DMF}\cdot 6\text{H}_2\text{O}\}_n$  (SNU-30):** We have prepared porous MOF **SNU-30** from the solvothermal reaction of *N,N,N',N'*-tetrakis(4-carboxyphenyl)biphenyl-4,4'-diamine ( $\text{H}_4\text{TCPBDA}$ ) and  $\text{Zn}(\text{NO}_3)_2\cdot 6\text{H}_2\text{O}$  in *N,N*-dimethylformamide (DMF)/*t*BuOH (5:1 v/v, 6 mL) at 80 °C for 24 h. The X-ray crystal structure studies of **SNU-30** reveal that the connectivity of square-shaped  $\{\text{Zn}_2(\text{O}_2\text{CR})_4\}$  secondary building units and the rectangular  $\text{TCPBDA}^{4-}$  ion gives rise to an NbO-type 3D framework, in which a water molecule is coordinated at the axial site of every  $\text{Zn}^{\text{II}}$  ion (Figure 1 and Table S1 in the Supporting Information). The phenyl rings around the nitrogen atoms in the  $\text{TCPBDA}^{4-}$  ion are twisted to each other with an average dihedral angle of 66.80(7)°. The framework generates 3D channels. Rhombic- and honeycomblike channels are generated on the *bc* and *ac* planes, respectively. Their effective aperture sizes are 10.7 × 17.4 and 13.8 × 17.5 Å<sup>2</sup>, respectively. On the *ab* plane, two different channels with rhombic- and honeycomblike apertures of effective sizes 2.7 × 3.8 and 5.1 × 10.5 Å<sup>2</sup>, respectively, are formed. The void volume of **SNU-30** is 82.1% (2.15 cm<sup>3</sup> g<sup>-1</sup>) and becomes 82.6% (2.17 cm<sup>3</sup> g<sup>-1</sup>) without the coordinated aqua ligands, as estimated by PLATON.<sup>[12]</sup> The calculated density of **SNU-30** is as

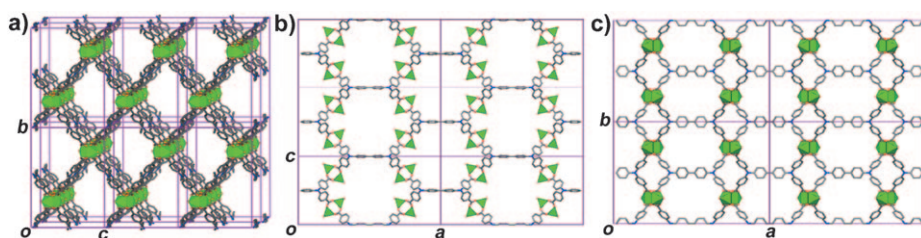


Figure 1. X-ray crystal structure of **SNU-30**. Views of the 3D framework seen on the a) *bc*, b) *ac*, and c) *ab* planes. Color scheme: Zn = green, C = gray, O = red, N = blue.

low as 0.381 g cm<sup>-3</sup> after removal of the guest and coordinated solvent molecules. Thermogravimetric analysis (TGA) suggests that the framework is thermally stable up to 300 °C (Figure S2 in the Supporting Information).

**SCSC transformation of SNU-30 on insertion of bpta linkers to afford  $[\text{Zn}_2(\text{TCPBDA})(\text{bpta})]\cdot 23\text{DMF}\cdot 4\text{H}_2\text{O}$  (SNU-31SC):** When the yellow crystal of **SNU-30** was immersed in a solution of bpta in DMF (0.033 M) at 80 °C for 3 hours, two coordinated water molecules in **SNU-30** were quantitatively substituted with a bpta molecule in **SNU-30**, thus resulting in a red crystal of  $\{[\text{Zn}_2(\text{TCPBDA})(\text{bpta})]\cdot 23\text{DMF}\cdot 4\text{H}_2\text{O}\}_n$  (**SNU-31SC**) by a SCSC transformation. Retention of the single crystallinity during the insertion of bpta was proven by photographs taken under a microscope (Figure 2).

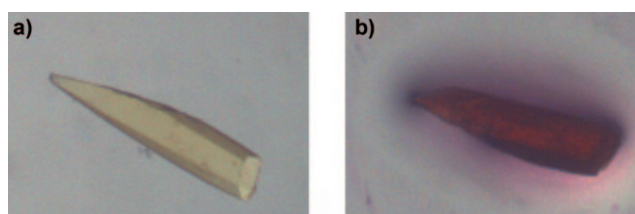


Figure 2. Photos of the **SNU-30** crystal a) before and b) after immersion in the solution of bpta (0.033 M) in DMF at 80 °C for 3 hours, which affords **SNU-31SC**.

The synchrotron X-ray crystal structure of **SNU-31SC** indicates that the bpta ligand connects  $\text{Zn}^{\text{II}}$  paddle-wheel units by maintaining the main framework structure of **SNU-30** (Figure 3). Interestingly, the bpta unit in **SNU-31SC** is sig-

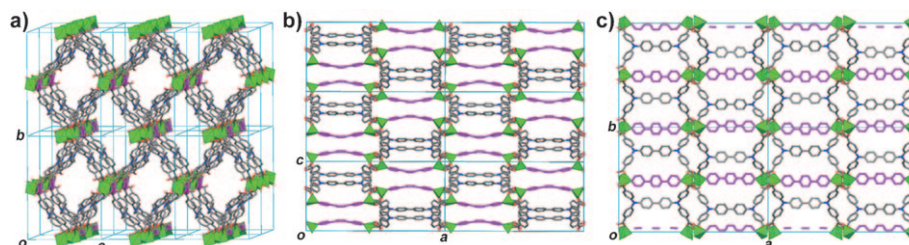


Figure 3. The X-ray crystal structure of **SNU-31SC**. Views seen on the a) *bc*, b) *ac*, c) *ab* planes. Color scheme: Zn = green, C = gray, O = red, N = blue, bpta linker = pink.

nificantly bent to fit into the  $\{\text{Zn}_2\}$  paddle-wheel units, contrary to the completely planar structure in a pristine bpta crystal (Figures S5 and S6 in the Supporting Information). The dihedral angle between the pyridyl rings is 19.53(23)° and that between the pyridine and tetrazine rings is 11.10(22)°. Rhombic cavities (effective

aperture size:  $18 \times 12 \text{ \AA}^2$ ) are formed, which are similar in size to those of **SNU-30**, on the *bc* plane. Due to the bent bpta ligand, dumbbell- and rectangular-shaped channels (effective aperture size:  $2.5 \times 14.6$  and  $2.6 \times 6.6 \text{ \AA}^2$ , respectively) are generated, the aperture sizes of which are significantly decreased relative to those of **SNU-30**, on the *ac* plane. The honeycomblike channels are divided into smaller rectangular channels (effective aperture size:  $1.1 \times 8.6 \text{ \AA}^2$ ) on the *ab* plane. The solvent-accessible volume of **SNU-31SC** is 76.1%, as estimated by PLATON.<sup>[12]</sup> The TGA data of **SNU-31SC** reveal 62.6% weight loss at 25–200 °C, which corresponds to the loss of all the guest solvent molecules (calcd: 63.0% for 23 DMF and 4 H<sub>2</sub>O molecules), and the additional weight loss of 8.8% at 230–380 °C, which corresponds to the loss of the bpta linker (calcd: 8.5%; Figure S8 in the Supporting Information).

The same compound as **SNU-31SC**,  $\{[\text{Zn}_2(\text{TCPBDA})\text{-}(\text{bpta})] \cdot 20 \text{ DMF} \cdot 4 \text{ H}_2\text{O}\}_n$  (**SNU-31**), was also synthesized from the solvothermal reactions of Zn<sup>II</sup>, H<sub>4</sub>TCPBDA, and bpta in DMF at 85 °C for 24 h (Scheme S2 in the Supporting Information). However, instead of the bpta ligand, when 4,4'-dipyridine (bpy), 1,2-bis(4-pyridyl)ethane (bpea), or *trans*-1,2-bis(4-pyridyl)ethylene (bpee) linkers were added to the reaction mixture, only **SNU-30** was formed because the lengths of bpy, bpea, and bpee (6.98, 9.21, and 9.19 Å, respectively) are too short to fit the two mutually parallel paddle-wheel units of the framework (Figure S3 in the Supporting Information). The X-ray crystal structure of **SNU-31** is very similar to that of **SNU-31SC**, and the bpta ligand is also significantly bent, although the space groups are different from each other, that is, *Imma* and *Pmnb*, respectively, as a result of the differences in the measurement temperature and the type of radiation. The TGA data of **SNU-31** indicate that the main framework is thermally stable up to 400 °C, although the bpta linkers are liberated at higher temperatures than 250 °C (Figure S11 in the Supporting Information).

**SCSC transformation of SNU-31 on removal of bpta linkers to afford SNU-30SC:** When the crystals of **SNU-31** or **SNU-31SC** were immersed in dried *N,N*-diethylformamide (DEF) for seven days at room temperature, the color of the crystals changed from red ( $\lambda_{\text{max}} = 340, 526 \text{ nm}$ ) to yellow ( $\lambda_{\text{max}} = 379 \text{ nm}$ ), and  $\{[\text{Zn}_2(\text{TCPBDA})(\text{H}_2\text{O})_2] \cdot 23 \text{ DEF}\}_n$  (**SNU-30SC**) was obtained with retention of the single crystallinity, as evidenced by photographs taken during the reaction (Figure 4). The X-ray crystal structure of **SNU-30SC** is very similar to that of **SNU-31**, from which **SNU-30SC** was

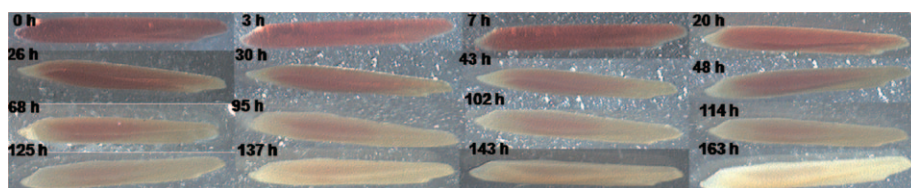


Figure 4. Photographs showing the SCSC transformation of **SNU-31** to **SNU-30SC** on removal of bpta linkers by immersion of **SNU-31** in DEF.

Table 1. Gas sorption data of **SNU-30'** and **SNU-31'**.

Gas	<i>T</i> [K]	<i>P</i> [atm]	Adsorption capacity			
			<b>SNU-30'</b>		<b>SNU-31'</b>	
			wt %	mmol gas per gram of host	wt %	mmol gas per gram of host
N <sub>2</sub>	77	0.9	27.0	9.67		<0.1
		1.0	1.42	7.04	0.20	0.51
H <sub>2</sub>	77	61	2.75 <sup>[a]</sup>	13.6 <sup>[a]</sup>		
			3.27 <sup>[b]</sup>	16.2 <sup>[b]</sup>		
O <sub>2</sub>	77	1.0	0.72	3.57		
		0.20	39.2	12.3		<0.1
CO <sub>2</sub>	87	0.61	39.1	12.2		
		1.0	46.2	10.5	17.2	3.90
		1.0	11.5	2.62	5.29	1.20
		1.0	5.12	1.16	2.62	0.60
CH <sub>4</sub>	298	50	21.9	4.98	9.41	2.14
		1.0	6.82	4.25	0.62	0.38
		1.0	1.32	0.82		
CH <sub>4</sub>	298	1.0	0.38	0.23		
		50	4.79	2.99	1.52	0.95

[a] Excess H<sub>2</sub> adsorption. [b] Total H<sub>2</sub> adsorption.

formed (Table 1 and Table S3 in the Supporting Information). The solvent-accessible volume of **SNU-30SC** is 82.7%, as estimated by PLATON,<sup>[12]</sup> similar to that of **SNU-30** (82.1%).

To the best of our knowledge, the present result is the first report of a SCSC transformation in which an organic linker is quantitatively and reversibly inserted to and removed from a 3D MOF without changing the main framework structure, although there are a few reports on the insertion of organic linker into a 2D layer or a polyhedron that led to a 3D MOF.<sup>[13,14]</sup>

**Gas-sorption properties of SNU-30' and SNU-31':** Desolvated solids  $[\text{Zn}_2(\text{TCPBDA})]_n$  (**SNU-30'**) and  $[\text{Zn}_2(\text{TCPBDA})\text{-}(\text{bpta})]_n$  (**SNU-31'**) were prepared by the heating-evacuation method to examine their gas-sorption properties (see the Experimental Section). **SNU-30'** and **SNU-31'** lost their transparency and single crystallinity. The powder X-ray diffraction (PXRD) patterns of **SNU-30'** and **SNU-31'** indicate that some structural changes occur on the removal of guest solvent molecules (Figures S18 and S19 in the Supporting Information). The supercritical CO<sub>2</sub> drying method also offered similar PXRD patterns.

The gas-adsorption isotherms of **SNU-30'** and **SNU-31'** were measured for N<sub>2</sub>, O<sub>2</sub>, H<sub>2</sub>, CH<sub>4</sub>, and CO<sub>2</sub> (adsorption data are compared in Table 1). **SNU-30'** adsorbs N<sub>2</sub>, showing a type-I isotherm that is characteristic for a microporous material (Figure 5a). The Langmuir and BET surface areas estimated from the N<sub>2</sub> gas-sorption data are 770 and 704 m<sup>2</sup>g<sup>-1</sup>, respectively. The pore volume estimated by using the Dubinin–Radushkevich (DR) equation is 0.28 cm<sup>3</sup>g<sup>-1</sup>. This surface area is significantly low relative to the theoretical values: 3924 m<sup>2</sup>g<sup>-1</sup> of Connolly

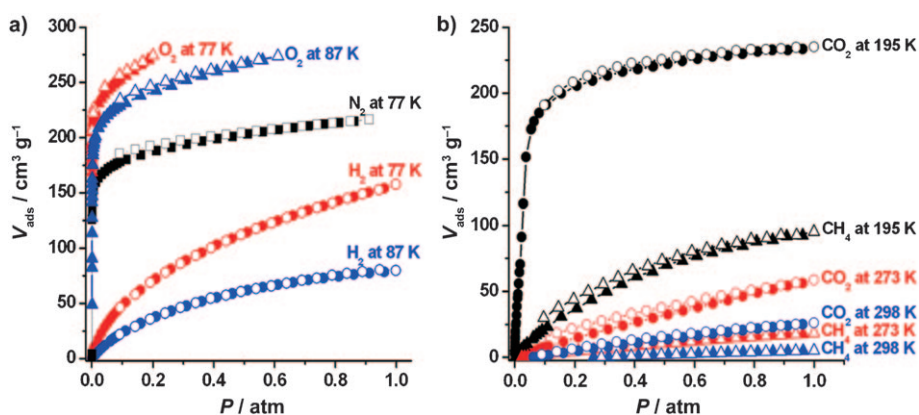


Figure 5. Gas-sorption isotherms of **SNU-30'**. a)  $\text{N}_2$  (■) at 77 K,  $\text{O}_2$  (▲) and  $\text{H}_2$  (●) at 77 (red) and 87 K (blue); b)  $\text{CO}_2$  (●) and  $\text{CH}_4$  (▲) at 195 (black), 273 (red), and 298 K (blue). Filled shapes: adsorption; open shapes: desorption.

surface area estimated by using the Materials Studio program<sup>[15]</sup> and  $5390 \text{ m}^2 \text{ g}^{-1}$  of the accessible surface area calculated from a simple Monte Carlo integration,<sup>[16]</sup> thus indicating that the framework is shrunken on desolvation. The plot of the pore-size distribution estimated by the Saito–Foley model<sup>[17]</sup> offers pore diameters of 10.5 and 11.8 Å (Figure S20 in the Supporting Information).

**SNU-30'** adsorbs 39.2 wt %  $\text{O}_2$  ( $275 \text{ cm}^3 \text{ g}^{-1}$  at STP) at 77 K and 0.20 atm and 39.1 wt %  $\text{O}_2$  ( $274 \text{ cm}^3 \text{ g}^{-1}$  at STP) at 87 K and 0.61 atm (Figure 5a). This  $\text{O}_2$  adsorption capacity at 77 K and 0.20 atm is comparable to those of **SNU-9** (51.4 wt %,  $360 \text{ cm}^3 \text{ g}^{-1}$ )<sup>[18]</sup> and **FMOF-1** (48 wt %,  $336 \text{ cm}^3 \text{ g}^{-1}$ )<sup>[19]</sup> but lower than the highest data ( $618 \text{ cm}^3 \text{ g}^{-1}$ ) for [Co(BDP)] (BDP=1,4-benzene di(4'pyrazolyl)).<sup>[20]</sup> The  $\text{O}_2$  adsorption densities in **SNU-30'**, estimated by using the pore volume derived from the  $\text{N}_2$  adsorption data, are  $1400 \text{ kg m}^{-3}$  at 77 K and 0.20 atm and  $1397 \text{ kg m}^{-3}$  at 87 K and 0.61 atm. This outcome suggests that  $\text{O}_2$  gas is highly compressed within the pores, given that the density of liquid  $\text{O}_2$  is  $1142 \text{ kg m}^{-3}$ .

**SNU-30'** adsorbs  $\text{H}_2$  gas up to 1.42 wt % ( $158 \text{ cm}^3 \text{ g}^{-1}$  at STP) at 77 K and 1 atm and 0.72 wt % of  $\text{H}_2$  ( $80 \text{ cm}^3 \text{ g}^{-1}$  at STP) at 87 K and 1 atm (Figure 5a). The isosteric heat of  $\text{H}_2$  adsorption for **SNU-30'** is 8.12–7.27  $\text{kJ mol}^{-1}$  depending on the degree of  $\text{H}_2$  loading, as estimated from the data at 77 and 87 K by using the virial equation (Figures S21 and S22 in the Supporting Information).<sup>[21]</sup> This isosteric heat of  $\text{H}_2$  adsorption is significantly higher than those of common MOFs, such as **MOF-5** (4.8  $\text{kJ mol}^{-1}$ )<sup>[22]</sup> due to the vacant coordination sites in **SNU-30'**. The excess and total  $\text{H}_2$  adsorption capacities at 77 K and 61 bar are 2.75 and 3.27 wt %, respectively (Figure S23 in the Supporting Information). However, the  $\text{H}_2$  adsorption capacity at 298 K and 71 bar becomes 0.16 wt %, similar to all other MOFs that show very low room-temperature  $\text{H}_2$  storage capacities.

The  $\text{CO}_2$  and  $\text{CH}_4$  adsorption isotherms of **SNU-30'** are presented in Figure 5b. **SNU-30'** adsorbs  $\text{CO}_2$  up to 46.2 wt % ( $235.19 \text{ cm}^3 \text{ g}^{-1}$  at STP) at 195 K and 1 atm and

11.5 wt % ( $58.63 \text{ cm}^3 \text{ g}^{-1}$  at STP) at 273 K and 1 atm. **SNU-30'** adsorbs 22.3 wt % of  $\text{CO}_2$  at 298 K and 45 bar (total: 25.5 wt %; Figure S24 in the Supporting Information). These values are similar to the  $\text{CO}_2$  adsorption capacity of 43.0 wt % at 195 K and 1 atm for **SNU-9**,<sup>[18]</sup> but lower than the highest value, namely, 149 wt % in **MOF-5** at 195 K and 1 atm.<sup>[23]</sup> The  $\text{CH}_4$  uptake capacities of **SNU-30'** are 6.82 wt % ( $95.18 \text{ cm}^3 \text{ g}^{-1}$  at STP) at 195 K and 1 atm ( $3.4 \text{ CH}_4$  molecules per formula unit) and 1.32 wt % ( $18.40 \text{ cm}^3 \text{ g}^{-1}$  at STP) at 273 K and 1 atm. **SNU-**

**30'** adsorbs an excess amount of  $\text{CH}_4$  up to 4.79 wt % at 298 K and 50 bar (total 6.21 wt %; Figure S24 in the Supporting Information). These  $\text{CH}_4$  capacities are relatively low compared with 21.8 wt % at 303 K and 60 bar for **MIL-101**<sup>[24]</sup> and 15.5 wt % at 298 K and 35 bar for **MOF-5**.<sup>[25]</sup>

Contrary to **SNU-30'**, **SNU-31'** hardly adsorbs  $\text{N}_2$ ,  $\text{H}_2$ ,  $\text{O}_2$ , and  $\text{CH}_4$  gases (Figure 6a). The X-ray structure of **SNU-31'** indicates that the channel sizes are big enough for these gases to enter (kinetic diameters: 3.64, 2.89, and 3.8 Å for  $\text{N}_2$ ,  $\text{H}_2$ , and  $\text{CH}_4$ , respectively), but the channels seem to be contracted on guest removal. Interestingly, however, **SNU-31'** adsorbs  $\text{CO}_2$ , which has a kinetic diameter of 3.3 Å, up to 12.9 wt % ( $65.7 \text{ cm}^3 \text{ g}^{-1}$  at STP) at 195 K and 1 atm (Figure 6a). This finding must be attributed to the quadrupole moment of  $\text{CO}_2$  ( $-1.34 \times 10^{-39} \text{ Cm}^2$ )<sup>[26]</sup> which induces stronger interaction with the framework than other gases. The desorption isotherm at 195 K shows a large hysteresis. The surface area and pore volume of **SNU-31'**, estimated from the  $\text{CO}_2$  adsorption isotherm by applying the DR equation, are  $308 \text{ m}^2 \text{ g}^{-1}$  and  $0.14 \text{ cm}^3 \text{ g}^{-1}$ , respectively. Relative to the theoretical values of the surface area (i.e.,  $3921 \text{ m}^2 \text{ g}^{-1}$  of Connolly surface area estimated by using the Materials Studio program<sup>[15]</sup> and  $4809 \text{ m}^2 \text{ g}^{-1}$  of the accessible surface area calculated from a simple Monte Carlo integration),<sup>[16]</sup> this surface area is remarkably lower, thus indicating that the framework is shrunken on desolvation. The  $\text{CO}_2$  sorption isotherms at 298 K exhibit adsorption capacities of 2.62 wt % at 1 atm and 9.83 wt % at 40 bar (Figure S25 in the Supporting Information). The MOF that selectively adsorbs  $\text{CO}_2$  over other gases can be applied in a  $\text{CO}_2$ -capture material from industrial flue gas.<sup>[2b]</sup> To verify the selective and reversible  $\text{CO}_2$  adsorption in **SNU-31'**, a gas-cycling experiment was performed in a TG pan with a flow of 15%  $\text{CO}_2$  in  $\text{N}_2$  (v/v) at 25 °C, which approximately mimics industrial flue gas, followed by a stream of pure  $\text{N}_2$  gas (Figure 6b). A reversible change of 0.32 wt % was observed over repeated cycles, and the material was regenerated by switching the gas stream to a  $\text{N}_2$  gas flow.

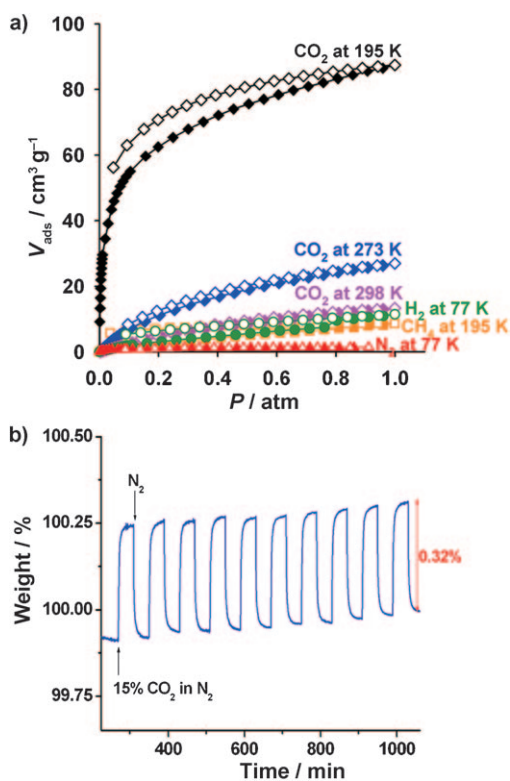


Figure 6. Selective  $\text{CO}_2$  sorption isotherms of SNU-31'. a)  $\text{CO}_2$  ( $\blacklozenge$ ) measured up to 1 atm at 195 (black), 273 (blue), and 298 K (pink) relative to adsorption isotherms for  $\text{N}_2$  ( $\blacktriangle$ ) and  $\text{H}_2$  ( $\bullet$ ) measured at 77 K and  $\text{CH}_4$  ( $\blacksquare$ ) measured at 195 K. Filled shapes: adsorption; open shapes: desorption. b) Gas-cycling experiment for SNU-31' at 25 °C with a flow of 15%  $\text{CO}_2$  in  $\text{N}_2$  (v/v) followed by a flow of pure  $\text{N}_2$ .

## Conclusion

We have demonstrated that a proper organic linker can be quantitatively and reversibly inserted into a MOF while maintaining single crystallinity to change the gas-sorption properties of the MOF. This type of post-synthetic modification could afford various new MOFs that could be applied in selective gas storage or gas separation.

## Experimental Section

**General methods:** All the chemicals and solvents used in the syntheses were of reagent grade and used without further purification. MeCN was dried by distillation over  $\text{P}_2\text{O}_5$  in a  $\text{N}_2$  atmosphere prior to use. DEF was dried over activated molecular sieves.  $\text{H}_4\text{TCPBDA}$  was prepared by modifying previously reported methods.<sup>[27]</sup> IR spectra were recorded on a Perkin–Elmer Spectrum One FTIR spectrophotometer. UV/Vis diffuse reflectance spectra were recorded on a Perkin–Elmer Lambda 35 UV/Vis spectrophotometer. Emission spectra were recorded on a Perkin–Elmer LS55 luminescence spectrophotometer. Elemental analyses were performed on a Perkin–Elmer 2400 series II CHN analyzer. TGA and differential scanning calorimetry (DSC) were performed in a  $\text{N}_2$  atmosphere at a scan rate of  $5^\circ\text{C min}^{-1}$  on TGA Q50 and DSC Q10 instruments (TA instruments), respectively. PXRD data were recorded on a Bruker D5005 diffractometer at 40 kV and 40 mA for  $\text{CuK}\alpha$  radiation ( $\lambda = 1.54050 \text{ \AA}$ ) at a scan speed of  $5^\circ\text{min}^{-1}$  and a step size of  $0.02^\circ$  in  $2\theta$ .

**Preparation of  $N,N,N',N'$ -tetrakis(4-bromophenyl)biphenyl-4,4'-diamine:**  $N,N,N',N'$ -tetraphenylbiphenyl-4,4'-diamine (2.0 g,  $4.0 \times 10^{-3}$  mol) was dissolved in  $\text{CHCl}_3$  (80 mL), and the solution in  $\text{CHCl}_3$  (20 mL) of  $\text{Br}_2$  (0.6 mL) was slowly added in an ice bath. After stirring at  $0^\circ\text{C}$  for 45 min, the mixture was added to hot EtOH (ca. 500 mL) and cooled to  $0^\circ\text{C}$  until a microcrystalline white precipitate of  $N,N,N',N'$ -tetrakis(4-bromophenyl)biphenyl-4,4'-diamine formed, which was filtered, washed with EtOH, and dried under reduced pressure (1.86 g, 58%).  $^1\text{H NMR}$  (300 MHz,  $\text{CDCl}_3$ ):  $\delta = 7.5$  (d, 4H), 7.4 (d, 8H), 7.1 (d, 4H), 7.0 ppm (d, 8H).

**Preparation of  $N,N,N',N'$ -tetrakis(4-carboxyphenyl)biphenyl-4,4'-diamine ( $\text{H}_4\text{TCPBDA}$ ):**  $N,N,N',N'$ -tetrakis(4-bromophenyl)biphenyl-4,4'-diamine (1.86 g,  $2.3 \times 10^{-3}$  mol) was dissolved in freshly distilled THF (80 mL), and  $n$ -butyllithium in hexane (20 mL, 1.6 M) was slowly added at  $-78^\circ\text{C}$ . After the mixture was stirred for 1 h, crushed dry ice was added to the solution from which a green precipitate immediately formed. Acetic acid was added to the greenish suspension for acidification until the precipitate disappeared. The resulting solution was added to mixture of water (ca. 500 mL) and MeOH (ca. 10 mL), from which a green–white precipitate was formed. The precipitate was recrystallized in MeOH/water, washed with water, and dried in a drying pistol (1.25 g, 80%).  $^1\text{H NMR}$  (300 MHz,  $[\text{D}_6]\text{DMSO}$ ):  $\delta = 7.8$  (d, 8H), 7.7 (d, 4H), 7.4 (d, 4H), 7.1 ppm (d, 8H); elemental analysis calcd (%) for  $[\text{H}_4\text{TCPBDA}]_2\cdot 2\text{H}_2\text{O}$  ( $\text{C}_{40}\text{H}_{32}\text{N}_2\text{O}_{10}$ ): C 68.57, H 4.60, N 4.00; found: C 68.25, H 4.44, N 3.80; FTIR (KBr pellet):  $\tilde{\nu} = 1688$  (O=C=O),  $1594 \text{ cm}^{-1}$ ; UV/Vis (0.1 M NaOH):  $\lambda_{\text{max}} = 347 \text{ nm}$ ; UV/Vis (diffuse reflectance):  $\lambda_{\text{max}} = 280 \text{ nm}$ ; luminescence (0.1 M NaOH):  $\lambda_{\text{max}} = 452 \text{ nm}$ ; solid luminescence:  $\lambda_{\text{max}} = 471 \text{ nm}$ .

**Solvothermal synthesis of  $\{[\text{Zn}_2(\text{TCPBDA})(\text{H}_2\text{O})_2]\cdot 30\text{DMF}\cdot 6\text{H}_2\text{O}\}_n$  (SNU-30):** A solution of  $\text{H}_4\text{TCPBDA}$  (32.2 mg, 0.05 mmol) in DMF (5 mL) and a solution of  $\text{Zn}(\text{NO}_3)_2\cdot 6\text{H}_2\text{O}$  (30.0 mg, 0.1 mmol) in  $t\text{BuOH}$  (1 mL) were mixed in a glass serum bottle, which was tightly capped with a silicon stopper and aluminum seal, and heated at  $80^\circ\text{C}$  for 24 h. The solution was cooled to room temperature, and the resulting yellow rod-shaped crystals were filtered and washed briefly with DMF (29.8 mg, 25%). Solid SNU-30 is insoluble in water and common organic solvents such as DMF, DEF,  $N,N$ -dimethylacetamide (DMA), EtOH, MeOH,  $t\text{BuOH}$ , and MeCN. Elemental analysis calcd (%) for  $\text{Zn}_2\text{C}_{120}\text{H}_{216}\text{N}_{26}\text{O}_{36}$ : C 50.98, H 8.23, N 14.63; found: C 51.12, H 8.01, N 14.73; FTIR (KBr pellet):  $\tilde{\nu} = 3432$  (O–H),  $1662$  (C=O (DMF)),  $1595 \text{ cm}^{-1}$  (O=C=O (TCPBDA)); UV/Vis (diffuse reflectance)  $\lambda_{\text{max}} = 350 \text{ nm}$ ; solid luminescence:  $\lambda_{\text{max}} = 472 \text{ nm}$ .

**Preparation of  $\{[\text{Zn}_2(\text{TCPBDA})(\text{bpta})]\cdot 23\text{DMF}\cdot 4\text{H}_2\text{O}\}_n$  (SNU-31SC) through the SCSC transformation of SNU-30 by the post-synthetic insertion of a bpta linker:** Single crystals of SNU-30 (36.2 mg, 0.012 mmol) were immersed in a solution of bpta (7.7 mg) in DMF (0.033 M, 1 mL) at  $80^\circ\text{C}$  for 3 h. The crystals changed from yellow to red with retention of single crystallinity, and crystals of  $\{[\text{Zn}_2(\text{TCPBDA})(\text{bpta})]\cdot 23\text{DMF}\cdot 4\text{H}_2\text{O}\}_n$  (SNU-31SC) were obtained, which were filtered and washed briefly with anhydrous DMF. If SNU-30 was immersed for longer period of time, bpta precipitated out and the crystallinity of SNU-31SC became poor. Interestingly, when the same reaction was carried out under different conditions, such as at room temperature with the same concentration of bpta or at  $80^\circ\text{C}$  with much more dilute solution of bpta ( $1.2 \times 10^{-3}$  M), the bpta ligand was not introduced into SNU-30 probably due to slow diffusion of bpta. To prove the maintenance of single crystallinity and exclude the possibility of dissolution and recrystallization during the bpta insertion, photographs of a single crystal were taken before and after immersion in the solution of bpta (7.7 mg) in DMF (0.033 M, 1 mL) at  $80^\circ\text{C}$  for 3 h. Elemental analysis calcd (%) for  $\text{Zn}_2\text{C}_{121}\text{H}_{201}\text{N}_{31}\text{O}_{31}$ : C 52.26, H 7.29, N 15.61; found: C 52.36, H 7.14, N 15.64; FTIR (KBr pellet):  $\tilde{\nu} = 3435$  (O–H),  $2927$  (C–H),  $1667$  (C=O (DMF)),  $1595 \text{ cm}^{-1}$  (O=C=O (TCPBDA)); UV/Vis (diffuse reflectance):  $\lambda_{\text{max}} = 527 \text{ nm}$ .

**Solvothermal synthesis of  $\{[\text{Zn}_2(\text{TCPBDA})(\text{bpta})]\cdot 20\text{DMF}\cdot 4\text{H}_2\text{O}\}_n$  (SNU-31):**  $\text{H}_4\text{TCPBDA}$  (32.2 mg, 0.05 mmol) and bpta (13.0 mg, 0.05 mmol) were dissolved in DMF (2 mL), and  $\text{Zn}(\text{NO}_3)_2\cdot 6\text{H}_2\text{O}$  (30.0 mg, 0.1 mmol) was dissolved in DMF (1 mL). The solutions were mixed and placed in a glass serum bottle, which was tightly capped with

a silicon stopper and aluminum seal, and heated at 85 °C for 24 h. The solution was cooled to room temperature, and the resulting red rod-shaped crystals were filtered and washed briefly with mother liquor. The formation of **SNU-31** is independent of the stoichiometry of the reactants (28.6 mg, 22.3%). Solid **SNU-31** is insoluble and stable in MeCN, *n*-hexane, *n*-dodecane, and toluene. Elemental analysis calcd (%) for  $Zn_2C_{112}H_{180}N_{28}O_{32}$ : C 52.52, H 7.08, N 15.31; found: C 52.17, H 7.43, N 15.16; FTIR (KBr pellet):  $\tilde{\nu}$  = 3430 (O–H), 2931 (C–H), 1660 (C=O (DMF)), 1595  $cm^{-1}$  (O–C=O (TCPBDA)); UV/Vis (diffuse reflectance):  $\lambda_{max}$  = 340, 526 nm.

**Preparation of  $\{[Zn_2(TCPBDA)(H_2O)_2] \cdot 23DEF\}_n$  (SNU-30SC) by the SCSC transformation of SNU-31 on removal of bpta:** Crystals of **SNU-31** were immersed in dried DEF at room temperature for 7 days. The crystals changed from red to yellow with retention of single crystallinity, which resulted the crystals of  $\{[Zn_2(TCPBDA)(H_2O)_2] \cdot 23DEF\}_n$  (**SNU-30SC**). However, when **SNU-31** was immersed for 7 days in another solvent, such as DMF or DMA, the single crystallinity was lost with the liberation of the bpta linkers. When the crystal was immersed in MeOH, EtOH, or *t*BuOH the whole framework dissociated. Elemental analysis calcd (%) for  $Zn_2C_{153}H_{281}N_{25}O_{33}$ : C 59.03, H 8.98, N 11.10; found: C 58.97, H 8.76, N 11.12; FTIR (KBr pellet):  $\tilde{\nu}$  = 3467 (O–H), 1661 (C=O (DEF)), 1595  $cm^{-1}$  (O–C=O (TCPBDA)); UV/Vis (diffuse reflectance):  $\lambda_{max}$  = 379 nm; solid luminescence:  $\lambda_{max}$  = 462 nm.

**Preparation of  $[Zn_2(TCPBDA)]_n$  (SNU-30’):** Compound **SNU-30** was heated in a Schlenk tube at 150 °C under vacuum for 24 h. Elemental analysis calcd (%) for  $Zn_2C_{40}H_{24}N_2O_8$ : C 60.70, H 3.06, N 3.54; found: C 59.16, H 3.16, N 3.47; FTIR (KBr pellet):  $\tilde{\nu}$  = 1598  $cm^{-1}$  (O–C=O (TCPBDA)); UV/Vis (diffuse reflectance):  $\lambda_{max}$  = 405 nm; solid luminescence:  $\lambda_{max}$  = 523 nm.

**Preparation of  $\{[Zn_2(TCPBDA)(bpta)] \cdot 20MeCN \cdot 5H_2O\}_n$  (SNU-31MeCN):** Crystals of **SNU-31** were immersed in anhydrous MeCN for one day, and then the solvent was replenished with fresh anhydrous MeCN. The crystals were immersed for another two days until all the DMF guest molecules were exchanged with MeCN. Elemental analysis calcd (%) for  $Zn_2C_{92}H_{102}N_{28}O_{13}$ : C 56.99, H 5.30, N 20.23; found: C 56.85, H 5.27, N 20.30; FTIR (KBr pellet):  $\tilde{\nu}$  = 2250 (C≡N (MeCN)), 1595  $cm^{-1}$  (O–C=O (TCPBDA)).

**Preparation of  $[Zn_2(TCPBDA)(bpta)]_n$  (SNU-31’):** Compound **SNU-31MeCN** was heated in a Schlenk tube at 70 °C under vacuum for 6 h. Elemental analysis calcd (%) for  $Zn_2C_{52}H_{32}N_8O_8$ : C 60.77, H 3.14, N 10.90; found: C 60.82, H 3.14, N 9.87; FTIR (nujol):  $\tilde{\nu}$  = 1597  $cm^{-1}$  (O–C=O (TCPBDA)); UV/Vis (diffuse reflectance):  $\lambda_{max}$  = 336, 545 nm.

**X-ray crystallography:** The diffraction data of **SNU-31SC** and the bpta crystal were measured at 100 K with synchrotron radiation ( $\lambda$  = 0.9000 Å) on a 6B MX-I ADSC Quantum-210 detector with a silicon (111) double-crystal monochromator at the Pohang Accelerator Laboratory (PAL), Korea. The crystals were coated with paratone oil to prevent the loss of guest molecules. The diffraction data were collected by using the omega scan method through a total rotation of 360°. The ADSC Quantum-210 ADX program (Ver. 1.96)<sup>[28]</sup> was used for data collection, and HKL2000 (Ver. 0.98.699)<sup>[29]</sup> was used for cell refinement, reduction, and absorption correction. For **SNU-30**, **SNU-31**, **SNU-30SC**, and **SNU-31MeCN**, each crystal was sealed in a glass capillary together with the mother liquor and the diffraction data

were collected at 298 K on an Enraf Nonius Kappa CCD diffractometer using graphite-monochromated  $MoK_{\alpha}$  radiation ( $\lambda$  = 0.71073 Å). Preliminary orientation matrices and unit-cell parameters were obtained from the peaks of the first ten frames and refined by using the complete data set. The frames were integrated and corrected for Lorentz and polarization effects by using DENZO.<sup>[29]</sup> Scaling and global refinement of the crystal parameters were performed using SCALEPACK.<sup>[29]</sup> The absorption corrections were made. The crystal structures were solved by the direct method<sup>[30]</sup> and refined by full-matrix least-squares refinement with the computer program SHELXL-97.<sup>[31]</sup> The positions of the non-hydrogen atoms were refined with anisotropic displacement factors. The hydrogen atoms were positioned geometrically by using a riding model. For all the samples, the guest molecules that occupy the channels could not be refined in the X-ray structure due to the severe disorder, and they were determined based on the IR spectra, elemental analysis, and TGA data. The electron densities of the disordered guest molecules were flattened by using the SQUEEZE option of PLATON.<sup>[12]</sup> The crystallographic data for **SNU-30**, **SNU-30SC**, **SNU-31**, **SNU-31SC**, **SNU-31MeCN**, and the bpta crystal are summarized in Table 2 (also Tables S1 and S2 in the Supporting Information). CCDC-769073 (**SNU-30**), CCDC-769074 (**SNU-30SC**), CCDC-769075 (**SNU-31**), CCDC-769076 (**SNU-31SC**), CCDC-769077 (**SNU-31MeCN**), and CCDC-769078 (bpta) contain the supplementary crystallographic data of this paper. These data can be obtained free of charge from The Cambridge Crystallographic Data Centre via [www.ccdc.cam.ac.uk/data\\_request/cif](http://www.ccdc.cam.ac.uk/data_request/cif).

**Low-pressure gas-sorption measurements:** The gas-sorption experiments were performed by using an automated micropore gas analyzer Autosorb-1 and Autosorb-3B (Quantachrome Instruments). The crystals of **SNU-30** and **SNU-31MeCN** as-synthesized were directly introduced to the gas-sorption apparatus and activated at 150 and 80 °C, respectively, under vacuum for 24 h to protect the desolvated solids from exposure to air. All the gases used were of 99.999% purity. The  $H_2$  and  $O_2$  gas-sorption isotherms were monitored at 77 and 87 K, and the  $CO_2$  and  $CH_4$  gas-sorption isotherms were measured at 195, 273, and 298 K at each equilibrium pressure by the static volumetric method. The weight of the sample was measured precisely after each gas-sorption measurement. The surface area and total pore volume for **SNU-30’** were determined from the  $N_2$  gas isotherm at 77 K. Multipoint BET and the Langmuir surface area were estimated by using the data recorded at  $P/P_0$  = 0.00057–

Table 2. Crystallographic data for **SNU-30**, **SNU-31SC**, **SNU-31**, **SNU-30SC**, and **SNU-31MeCN** (squeezed).<sup>[a]</sup>

	<b>SNU-30</b>	<b>SNU-31SC</b>	<b>SNU-31</b>	<b>SNU-30SC</b>	<b>SNU-31MeCN</b>
formula	$Zn_2C_{40}H_{28}N_2O_{10}$	$Zn_2C_{52}H_{32}N_8O_8$	$Zn_2C_{52}H_{32}N_8O_8$	$Zn_2C_{40}H_{28}N_2O_{10}$	$Zn_2C_{52}H_{32}N_8O_8$
space group	<i>Imma</i>	<i>Pnmb</i>	<i>Imma</i>	<i>Imma</i>	<i>Imma</i>
$M_r$	827.43	1027.63	1027.63	827.43	1027.63
$a$ [Å]	35.965(7)	34.103(7)	34.158(7)	34.583(7)	34.277(7)
$b$ [Å]	23.273(5)	23.758(5)	22.850(5)	22.915(5)	23.356(5)
$c$ [Å]	17.219(3)	17.033(3)	19.049(4)	18.833(4)	18.400(4)
$V$ [Å <sup>3</sup> ]	14412.5(11)	13800(5)	14868(5)	14925(5)	14730(5)
$Z$	4	4	4	4	4
$\rho_{calcd}$ [g cm <sup>-3</sup> ]	0.381	0.495	0.459	0.368	0.463
$T$ [K]	298	100	298	298	298
$\lambda$ [Å]	0.71073	0.9000	0.71073	0.71073	0.71073
$\mu$ [mm <sup>-1</sup> ]	0.349	0.370	0.343	0.337	0.346
GOF ( $F^2$ )	0.985	0.918	0.766	0.776	0.922
$R_1, wR_2$	0.0693 <sup>[b]</sup> , 0.1973 <sup>[c]</sup>	0.0702 <sup>[b]</sup> , 0.1816 <sup>[d]</sup>	0.0522 <sup>[b]</sup> , 0.1177 <sup>[e]</sup>	0.0678 <sup>[b]</sup> , 0.1864 <sup>[f]</sup>	0.0742 <sup>[b]</sup> , 0.1917 <sup>[g]</sup>
$R_1, wR_2$ (all data)	0.1121 <sup>[b]</sup> , 0.2045 <sup>[c]</sup>	0.0917 <sup>[b]</sup> , 0.1897 <sup>[d]</sup>	0.1422 <sup>[b]</sup> , 0.1332 <sup>[e]</sup>	0.1254 <sup>[b]</sup> , 0.1967 <sup>[f]</sup>	0.1001 <sup>[b]</sup> , 0.2020 <sup>[g]</sup>

[a] As a result of the severe disorder of the guest molecules only the coordinating  $H_2O$  molecules and bpta linkers were refined for **SNU-30/SNU-30SC** and **SNU-31/SNU-31SC**, respectively. [b]  $R = \sum ||F_o| - |F_c|| / \sum |F_o|$ . [c]  $wR(F^2) = [\sum w(F_o^2 - F_c^2)^2 / \sum w(F_o^2)^2]^{1/2}$  where  $w = 1/[\sigma^2(F_o^2) + (0.0952P)^2 + (0.0000)P]$ ,  $P = (F_o^2 + 2F_c^2)/3$  for **SNU-30**. [d]  $wR(F^2) = [\sum w(F_o^2 - F_c^2)^2 / \sum w(F_o^2)^2]^{1/2}$  where  $w = 1/[\sigma^2(F_o^2) + (0.1295P)^2 + (0.0000)P]$ ,  $P = (F_o^2 + 2F_c^2)/3$  for **SNU-31SC**. [e]  $wR(F^2) = [\sum w(F_o^2 - F_c^2)^2 / \sum w(F_o^2)^2]^{1/2}$  where  $w = 1/[\sigma^2(F_o^2) + (0.0579P)^2 + (0.0000)P]$ ,  $P = (F_o^2 + 2F_c^2)/3$  for **SNU-31**. [f]  $wR(F^2) = [\sum w(F_o^2 - F_c^2)^2 / \sum w(F_o^2)^2]^{1/2}$  where  $w = 1/[\sigma^2(F_o^2) + (0.0994P)^2 + (0.0000)P]$ ,  $P = (F_o^2 + 2F_c^2)/3$  for **SNU-30SC**. [g]  $wR(F^2) = [\sum w(F_o^2 - F_c^2)^2 / \sum w(F_o^2)^2]^{1/2}$  where  $w = 1/[\sigma^2(F_o^2) + (0.1315P)^2 + (0.0000)P]$ ,  $P = (F_o^2 + 2F_c^2)/3$  for **SNU-31MeCN**.

0.093 atm and 0.00057–0.11 atm, respectively. The surface area and pore volume for SNU-31' were estimated from the CO<sub>2</sub> gas isotherm at 195 K by applying the DR equation.

**High-pressure gas-sorption measurements:** High-pressure gas-sorption isotherms for H<sub>2</sub>, CO<sub>2</sub>, and CH<sub>4</sub> were measured on a Rubotherm magnetic suspension balance (MSB) apparatus by using the gravimetric method. All the gases used were of 99.999% purity and the impurity trace water was removed by passing the gases through the drying trap (model 500) filled with molecular sieves (5 Å), which were purchased from Chromatography Research Supplies (CRS). SNU-30' and SNU-31' were prepared by heating crystals of SNU-30 and SNU-31MeCN at 150 and 80 °C, respectively, under vacuum for 24 h by using a Schlenk line, and they were activated again in the apparatus by evacuation at 150 °C and 80 °C, respectively. The H<sub>2</sub> sorption isotherms were measured at 77 and 298 K. The CO<sub>2</sub> and CH<sub>4</sub> sorption isotherms were measured at 298 K. To obtain the excess adsorption isotherm, all the data were corrected for buoyancy of the system and the sample. The sample density used for buoyancy correction was determined from the He displacement isotherm (up to 100 bar) measured at 298 K. The total amount of gas adsorbed was calculated by using Equation (1):<sup>[32,1b]</sup>

$$C_{\text{total}} = C_{\text{excess}} + (V_{\text{pore}} \times d_{\text{gas}} \times 100) \quad (1)$$

where  $C_{\text{total}}$  is the total adsorbed amount (wt%),  $C_{\text{excess}}$  is the excess adsorbed amount (wt%) on the surface,  $V_{\text{pore}}$  is the pore volume (cm<sup>3</sup>g<sup>-1</sup>) calculated from the N<sub>2</sub> gas sorption, and  $d_{\text{gas}}$  is the density of the compressed gas as a function of temperature and pressure (gcm<sup>-3</sup>).<sup>[33]</sup>

**Gas-cycling experiment for SNU-31':** Prior to the gas-cycling experiment, SNU-31MeCN was pre-desolvated in a Schlenk tube by heating at 70 °C under vacuum for 6 h. The pre-desolvated sample was introduced to the TGA Q50. Prior to gas cycling, the sample was reactivated by heating at 70 °C for 3 h followed by cooling to 25 °C in a nitrogen atmosphere. The CO<sub>2</sub> gas-cycling experiments were performed by using a flow of 15% CO<sub>2</sub> in N<sub>2</sub> (v/v), followed by a flow of pure N<sub>2</sub> (99.9999%). A flow rate of 60 mLmin<sup>-1</sup> was employed for both gases.

## Acknowledgements

This work was supported by the National Research Foundation of Korea (NRF) through a grant funded by the Korean Government (MEST) (No. 2009-0093842 and No. 2010-0001485). H.J.P. acknowledges support from the Seoul Science Fellowship. The authors acknowledge Pohang Accelerator Laboratory (PAL) for synchrotron beamline use.

- [1] a) L. J. Murray, M. Dincă, J. R. Long, *Chem. Soc. Rev.* **2009**, *38*, 1294–1314; b) S. S. Kaye, A. Dailly, O. M. Yaghi, *J. Am. Chem. Soc.* **2007**, *129*, 14176–14177; c) M. Latroche, S. Surble, C. Serre, F. Millange, G. Férey, *Angew. Chem.* **2006**, *118*, 8407–8411; *Angew. Chem. Int. Ed.* **2006**, *45*, 8227–8231; d) S. Yang, X. Lin, A. J. Blake, G. S. Walker, P. Hubberstey, N. R. Champness, M. Schröder, *Nat. Chem.* **2009**, *1*, 487–493.
- [2] a) Y. E. Cheon, M. P. Suh, *Angew. Chem.* **2009**, *121*, 2943–2947; *Angew. Chem. Int. Ed.* **2009**, *48*, 2899–2903; b) H.-S. Choi, M. P. Suh, *Angew. Chem.* **2009**, *121*, 6997–7001; *Angew. Chem. Int. Ed.* **2009**, *48*, 6865–6869; c) Y.-G. Lee, H. R. Moon, Y. E. Cheon, M. P. Suh, *Angew. Chem.* **2008**, *120*, 7855–7859; *Angew. Chem. Int. Ed.* **2008**, *47*, 7741–7745.
- [3] a) J.-R. Li, R. J. Kuppler, H.-C. Zhou, *Chem. Soc. Rev.* **2009**, *38*, 1477–1504; b) Y. E. Cheon, M. P. Suh, *Chem. Commun.* **2009**, 2296–2298; c) Y. E. Cheon, J. Park, M. P. Suh, *Chem. Commun.* **2009**, 5436–5438; d) H. R. Moon, N. Kobayashi, M. P. Suh, *Inorg. Chem.* **2006**, *45*, 8672–8676; e) L. Pan, D. H. Olson, L. R. Ciemnomolonski, R. Heddy, J. Li, *Angew. Chem.* **2006**, *118*, 632–635; *Angew. Chem. Int. Ed.* **2006**, *45*, 616–619.
- [4] a) T. Uemura, R. Kitaura, Y. Ohta, M. Nagaoka, S. Kitagawa, *Angew. Chem.* **2006**, *118*, 4218–4222; *Angew. Chem. Int. Ed.* **2006**, *45*, 4112–4116; b) M. Banerjee, S. Das, M. Yoon, H. J. Choi, M. H. Hyun, S. M. Park, G. Seo, K. Kim, *J. Am. Chem. Soc.* **2009**, *131*, 7524–7525; c) C. D. Wu, A. Hu, L. Zhang, W. Lin, *J. Am. Chem. Soc.* **2005**, *127*, 8940–8941.
- [5] a) H. R. Moon, J. H. Kim, M. P. Suh, *Angew. Chem.* **2005**, *117*, 1287–1291; *Angew. Chem. Int. Ed.* **2005**, *44*, 1261–1265; b) Y. E. Cheon, M. P. Suh, *Chem. Eur. J.* **2008**, *14*, 3961–3967; c) F. Schröder, D. Esken, M. Cokoja, M. W. E. van den Berg, O. I. Lebedev, G. Van Tendeloo, B. Walaszek, G. Buntkowsky, H.-H. Limbach, B. Chaudret, R. A. Fischer, *J. Am. Chem. Soc.* **2008**, *130*, 6119–6130; d) C. Liang, W. Xia, M. van den Berg, Y. Wang, H. Soltani-Ahmadi, O. Schluter, R. A. Fischer, M. Muhler, *Chem. Mater.* **2009**, *21*, 2360–2366.
- [6] M. P. Suh, H. R. Moon, E. Y. Lee, S. Y. Jang, *J. Am. Chem. Soc.* **2006**, *128*, 4710–4718.
- [7] a) Z. Wang, S. M. Cohen, *J. Am. Chem. Soc.* **2009**, *131*, 16675–16677; b) S. C. Jones, C. A. Bauer, *J. Am. Chem. Soc.* **2009**, *131*, 12516–12517; c) K. M. L. Taylor-Pashow, J. D. Rocca, Z. Xie, S. Tran, W. Lin, *J. Am. Chem. Soc.* **2009**, *131*, 14261–14263; d) W. Morris, C. J. Doonan, H. Furukawa, R. Banerjee, O. M. Yaghi, *J. Am. Chem. Soc.* **2008**, *130*, 12626–12627.
- [8] a) M. P. Suh, J. W. Ko, H. J. Choi, *J. Am. Chem. Soc.* **2002**, *124*, 10976–10977; b) E. Y. Lee, S. Y. Jang, M. P. Suh, *J. Am. Chem. Soc.* **2005**, *127*, 6374–6381; c) E. Y. Lee, M. P. Suh, *Angew. Chem.* **2004**, *116*, 2858–2861; *Angew. Chem. Int. Ed.* **2004**, *43*, 2798–2801; d) H. J. Park, M. P. Suh, *Chem. Eur. J.* **2008**, *14*, 8812–8821; e) M. P. Suh, Y. E. Cheon, E. Y. Lee, *Chem. Eur. J.* **2007**, *13*, 4208–4215.
- [9] a) K. Takaoka, M. Kawano, M. Tominaga, M. Fujita, *Angew. Chem.* **2005**, *117*, 2189–2192; *Angew. Chem. Int. Ed.* **2005**, *44*, 2151–2154; b) S. M. Neville, B. Mouvaraki, K. Murray, C. J. Kepert, *Angew. Chem.* **2007**, *119*, 2105–2108; *Angew. Chem. Int. Ed.* **2007**, *46*, 2059–2062.
- [10] a) T. Kawamichi, T. Kodama, M. Kawano, M. Fujita, *Angew. Chem.* **2008**, *120*, 8150–8152; *Angew. Chem. Int. Ed.* **2008**, *47*, 8030–8032; b) C.-D. Wu, W. Lin, *Angew. Chem.* **2005**, *117*, 1994–1997; *Angew. Chem. Int. Ed.* **2005**, *44*, 1958–1961.
- [11] H. J. Choi, M. P. Suh, *J. Am. Chem. Soc.* **2004**, *126*, 15844–15851.
- [12] A. L. Spek, PLATON99, A Multipurpose Crystallographic Tool, Utrecht University, Utrecht, **1999**.
- [13] a) R. Kitaura, F. Iwahori, R. Matsuda, S. Kitagawa, Y. Kubota, M. Takata, T. C. Kobayashi, *Inorg. Chem.* **2004**, *43*, 6522–6524; b) L. Pan, H. Liu, S. P. Kelly, X. Huang, D. H. Olson, J. Li, *Chem. Commun.* **2003**, 854–855.
- [14] J.-R. Li, D. J. Timmons, H.-C. Zhou, *J. Am. Chem. Soc.* **2009**, *131*, 6368–6369.
- [15] Materials Studio program, version 4.1, Accelrys, San Diego, **2006**.
- [16] T. Düren, F. Millange, G. Férey, K. S. Walton, R. Q. Snurr, *J. Phys. Chem. C* **2007**, *111*, 15350–15356.
- [17] A. Saito, H. C. Foley, *AIChE J.* **1991**, *37*, 429–436.
- [18] H. J. Park, M. P. Suh, *Chem. Commun.* **2010**, 46, 610–612.
- [19] C. Yang, X. Wang, M. A. Omary, *J. Am. Chem. Soc.* **2007**, *129*, 15454–15455.
- [20] H. J. Choi, M. Dincă, J. R. Long, *J. Am. Chem. Soc.* **2008**, *130*, 7848–7850.
- [21] L. Czepirski, J. Jagiello, *Chem. Eng. Sci.* **1989**, *44*, 797–801.
- [22] J. L. C. Rowsell, O. M. Yaghi, *J. Am. Chem. Soc.* **2006**, *128*, 1304–1315.
- [23] K. S. Walton, A. R. Millward, D. D. Houston, F. J. J. Low, O. M. Yaghi, R. Q. Snurr, *J. Am. Chem. Soc.* **2008**, *130*, 406–407.
- [24] P. L. Llewellyn, S. Bourrelly, C. Serre, A. Vimont, M. Daturi, L. Hamon, G. D. Weirald, J.-S. Chang, D.-Y. Hong, Y. K. Hwang, S. H. Jung, G. Férey, *Langmuir* **2008**, *24*, 7245–7250.
- [25] T. Düren, L. Sarkisov, O. M. Yaghi, R. Q. Snurr, *Langmuir* **2004**, *20*, 2683–2689.
- [26] a) Y.-S. Bae, K. L. Mulfort, H. Frost, S. Punnathanam, L. J. Broadbelt, J. T. Hupp, R. Q. Snurr, *Langmuir* **2008**, *24*, 8592–8598; b) S.

- Coriani, A. Halkier, A. Rizzo, K. Ruud, *Chem. Phys. Lett.* **2000**, 326, 269–276.
- [27] a) S. Dapperheld, E. Steckhan, K.-H. G. Brinkhaus, T. Esch, *Chem. Ber.* **1991**, 124, 2557–2567; b) E. W. Reynolds, K. T. Lorenz, H. S. Chiou, D. J. Bellville, R. A. Pabon, N. L. Bauld, *J. Am. Chem. Soc.* **1987**, 109, 4960–4968.
- [28] A. J. Arvai, C. Nielsen, ADSC Quantum-210 ADX Program, Area Detector System Corporation, Poway, **1983**.
- [29] Z. Otwinowski, W. Minor in *Processing of X-ray Diffraction Data Collected in Oscillation Mode, Methods in Enzymology, Vol. 276, Part A* (Eds.: C. W. Carter, Jr., R. M. Sweet), Academic Press, New York, **1997**, p. 307.
- [30] G. M. Sheldrick, *Acta Crystallogr. Sect. A* **1990**, 46, 467–473.
- [31] G. M. Sheldrick, SHELXL97, Program for the crystal structure refinement, University of Göttingen, Göttingen, **1997**.
- [32] H. Furukawa, M. A. Miller, O. M. Yaghi, *J. Mater. Chem.* **2007**, 17, 3197–3204.
- [33] NIST chemistry webbook (thermophysical properties of fluid systems): <http://webbook.nist.gov/chemistry/fluid/>.

Received: June 3, 2010

Published online: September 8, 2010